Tuning the reactivity of chelated dinuclear Pt(II) complexes through a flexible diamine linker. A detailed kinetic and mechanistic study†

Allen Mambanda,[a] Deogratius Jaganyi,*[a] Stephanie Hochreuther[b] and Rudi van Eldik*[b]

Received 16th October 2009, Accepted 15th January 2010
First published as an Advance Article on the web 12th February 2010
DOI: 10.1039/b921687a

The rate of displacement of the aqua ligands by three neutral nucleophiles (Nu) of different steric demands, namely thiourea (tu), *N*,*N*′-dimethylthiourea (dmtu) and *N*,*N*,*N*′,*N*′-tetramethylthiourea (tmtu) and an anionic nucleophile (I^-) in complexes of the form [{Pt(H_2O)}$_2$(*N*,*N*,*N*′,*N*′-tetrakis(2-pyridylmethyl)-N(CH_2)$_n$N](CF_3SO_3)$_4$, $n = 2$ (**En**); 3 (**Prop**); 4 (**But**); 6 (**Hex**); 8 (**Oct**) and 10 (**Dec**), was studied under pseudo first-order conditions as a function of concentration, temperature and pressure using stopped-flow techniques and UV-visible spectrophotometry. The pseudo first-order rate constants, $k_{obs(1^{st}/2^{nd})}$, for the simultaneous substitution of the aqua ligands and the proposed subsequent dechelation of the pyridyl units, respectively, agreed well to the rate law: $k_{obs(1^{st}/2^{nd})} = k_{2(1^{st}/2^{nd})}$[Nu]. High negative activation entropies, negative volumes of activation and second-order kinetics for the displacement reactions all support an associative mode of activation. Except for **Prop**, the rate of the simultaneous substitution of the aqua ligands in the complexes was found to increase as the chain length of the linker increases from **En** to **Hex**, beyond which any further increase in chain length is not accompanied by a further increase in reactivity. The reactivity trend of the even-bridged complexes with C_{2h} symmetry is ascribed to a concomitant decrease in axial steric influences imposed on one side of the square-planar picolyl chelates by the other as the chain length increases. Based on the model structures of the complexes, this kind of steric imposition occurs only in complexes with an even number of CH_2 groups within the linker. The **Prop** complex, having a C_{2v} symmetry showed exceptional high reactivity towards the nucleophiles. A cage effect, evolving from its bowl-shaped molecular structure, is proposed to explain this high reactivity. The order of reactivity of the nucleophiles increased in the order $I^- \gg$ tu ≈ dmtu > tmtu, in line with the strong electrostatic interactions between the highly polarizable iodide nucleophile and the Pt centers, steric retardation effects in the case of tmtu and dominating positive inductive effects for the dmtu nucleophile.

Introduction

The interaction of platinum based drugs with DNA is now widely accepted as the mechanism responsible for their anticancer activity.[1-4] Multinuclear Pt(II) complexes synthesized first by Farrell and his group,[5-8] can form a wide variety of DNA adducts through their diversified structural properties. Specifically, the length of the diamine linker is known to control the relative amounts of interstrand/intrastrand DNA crosslinks that can be formed by the complexes.[6] This confers them with a wide span of activities relative to the most successful mononuclear anticancer drugs, *viz.*, cisplatin, carboplatin and oxaliplatin.

The most successful representative of this class of complexes is BBR3464, [μ-*trans*-Pt(NH_3)$_2${*trans*-PtCl(NH_3)$_2$-NH_2(CH_2)$_6$$NH_2$}$_2$]($NO_3$)$_4$, a trinuclear complex with monodentate amine ligands around the Pt centers. It shows remarkable cytotoxicity against pancreatic, lung and melanoma cancers and has already entered phase two of the clinical trials.[9] It has a therapeutic index that is comparable to cisplatin and shows a remarkable lack of resistance in cisplatin-insensitive cell lines.[10] However, it has emerged from the results of recent studies,[7,11,12] that BBR3464 and its analogues, which have monodentate amine ligands around the platinum centers and leaving groups of *trans* geometry to the alkanediamine linker, can be degraded *in vitro* via liberation of the alkanediamine bridge. This happens when strong *trans*-effect ligands like the sulfur containing bio-molecules, whose *in vivo* prevalence is quite notable, substitute the leaving groups on the Pt centers.

Besides this, data in literature lacks coherence in terms of how the bridging diamine linker controls the reactivity of the Pt centers in multinuclear complexes. Recent studies have shown a general increase in reactivity of some α,ω-alkanediamine-bridged dinuclear Pt(II) complexes with monodentate[13] amines and bis(2-pyridylmethyl)amine[14] carrier ligands around the Pt centers. This happens when the chain length of the α,ω-alkanediamine, a measure of the average distance between their coordination spheres, is

[a]*School of Chemistry, University of KwaZulu-Natal, Scottsville 3209, Pietermaritzburg, South Africa*
[b]*Department of Chemistry and Pharmacy, University of Erlangen-Nürnberg, Egerlandstraße 1, 91058, Erlangen, Germany*

† Electronic supplementary information (ESI) available: A summary of wavelengths used for kinetics; spectral changes for a titration of **Oct** with NaOH, a kinetic trace showing the two reaction steps for a reaction mixture of tu (3 mM) and **bpma**; ^{1}H NMR spectral arrays (aromatic protons only) for the reaction between tu and **Dec**; exemplary Tables of data and the respective plots showing the dependence of $k_{obs(1^{st}/2^{nd})}$ on concentration of nucleophiles, temperature and pressure of the system for some selected complexes and the model structures for **Pen** and **Hep**. See DOI: 10.1039/b921687a

reduced.[14] The increase in reactivity was ascribed to an increase in charge addition of the Pt atoms caused by a combination of increased electrostatic interactions with concomitant reduction in the σ-donor capacity towards each Pt atom. In three separate kinetic studies, van Eldik and co-workers[14a-c] studied the substitution of aqua ligands in alkanediamine-bridged dinuclear complexes with a bis(2-pyridylmethyl)amine chelate framework around each Pt atom using anionic[14a,b] and biologically relevant[14c] nucleophiles. In all cases, they reported a similar trend in reactivity as reported by Jaganyi *et al.*[13] for the dinuclear complexes with monodentate amine ligands around the Pt(II) centers. The interactions or lack of it, occurring between the two Pt(II) centers, were found to correlate with the average Pt–Pt distance between them, becoming weaker as the alkanediamine chain length increases. Interestingly, the combined results of the three studies,[14a-c] clearly indicate that complexes bearing alkanediamine bridges with an odd number of CH_2 groups ($n = 3, 5, 7$) have a superior reactivity gradient per unit increase in CH_2 groups when compared to complexes bridged by an even number of CH_2 groups. This trend has not been fully understood.

More so, a substitution mechanism in which the second observed step is in fact a ring-opening process has been proposed for the decane-bridged complex, in which one of the *cis*-positioned pyridyl arms of the picolyl unit is decoordinated from the Pt(II) centers. This is well supported by ^{195}Pt NMR data.[14c] However, should this be happening as proposed, it may imply that all the other complexes would necessary undergo dechelation in their second observed steps bearing in mind reactivity had been reported to increase inversely with chain length according to two of the previous studies. Even though the linkers of the complexes were not completely liberated from the Pt atoms as reported for complexes studied by Summa *et al.*,[11] the results imply that the bis(2-pyridylmethyl)amine chelate core carrier ligand, is partially prone to *cis*-substitutional labilization *via* dechelation of the picolyl arms by the strong sulfur nucleophiles. However, data available in literature[15,16a] from other studies for the reactions between the sulfur containing nucleophiles and chelated Pt(II) complexes clearly shows that chelation can mitigate the problem of labilization of the *trans*-donor atoms by incoming sulfur containing molecules. In addition, increased chelation at a monomeric Pt(II) center has been shown to enhance reactivity[16b,c] apart from conferring thermodynamic stability.[16d]

One of the many challenges limiting an adequate understanding of the role of the bridging linker on the reactivity of multinuclear Pt(II) complexes is its concomitant structural complexity. The linker serves as an integral part of the core backbone of the carrier ligand framework around each Pt(II) center as well as being the linking structural entity between the Pt(II) centers. It also confers special structural properties on the metal complexes such as structural flexibility (as in an alkanediamine[5-6] linker) and structural rigidity (as in azines,[17] azoles[18] and the dipyrazolylmethane[19]). To gain a full understanding of possible factors controlling reactivity at square-planar Pt(II) centers in multinuclear complexes, one has to perform a systematic study in which all the other structural features within the series of complexes under study are kept constant while the feature of interest is varied.

We report on the influence of the bridging alkanediamine linker in dinuclear Pt(II) complexes with a bis(picolyl)amine chelate backbone. The picolyl π-acceptor fragments do not have an 'electronic linkage'[20] between them since their combined π-conjugation framework is not extended. To accomplish our objectives, we set out to synthesize six complexes of the type, $[\{Pt(H_2O)\}_2(N,N,N',N'$-tetrakis(2-pyridylmethyl)-$N(CH_2)_nN](CF_3SO_3)_4$, $n = 2$ (**En**); 3 (**Prop**); 4 (**But**); 6 (**Hex**); 8 (**Oct**) and 10 (**Dec**). All except **Prop** have even numbers of CH_2 groups in their alkanediamine bridge. The monomeric analogue to these complexes, $[Pt(H_2O)(N,N$-bis(2-pyridylmethyl)amine$](CF_3SO_3)_2$, (**bpma**) was also studied under the same experimental conditions.

Experimental

Preparation of ligands

Ligands **LI** to **L6**, were synthesized following the literature method of Sato *et al.*[21] *N*,*N*,*N*′,*N*′-tetrakis(2-pyridylmethyl)-1,2-ethanediamine (**LI**); *N*,*N*,*N*′,*N*′-tetrakis(2-pyridylmethyl)-1,3-propanediamine (**L2**); *N*,*N*,*N*′,*N*′-tetrakis(2-pyridylmethyl)-1,4-butanediamine (**L3**); *N*,*N*,*N*′,*N*′-tetrakis(2-pyridylmethyl)-1,6-hexanediamine (**L4**); *N*,*N*,*N*′,*N*′-tetrakis(2-pyridylmethyl-1,8-octanediamine (**L5**) and *N*,*N*,*N*′,*N*′-tetrakis(2-pyridylmethyl)-1,10-decanediamine (**L6**).

Colorless crystals (X-ray quality) in the case of **L1**, **L2**, **L3** and **L6** were obtained from solutions of ethanol by slow evaporation of the solvent over several days. The other ligands were collected as microcrystalline powders from a suspension of the oils in ethanol. The identity and purity of the compounds was further confirmed by ^{1}H NMR, ^{13}C NMR, TOF MS-ES$^+$ micro analysis and Infrared (IR). The IR spectra of the ligands showed common characteristic peaks at the following frequencies cm^{-1}: 2937 (broad, medium, C_{sp^3}-H stretch); 1589 (sharp and strong, $C_{sp^2} = N$ stretch, pyridyl rings).

(**L1**) Yield: 985 mg (77%). ^{1}H NMR (500 MHz, CD_3OD) δ (ppm): 8.39 (td, 4H); 7.72 (td, 4H); 7.52 (d, 4H); 7.25 (td, 4H); 3.31 (m, 4H); 2.69 (s, 8H). IR (KBr, 4000-400 cm^{-1}) $\bar{\nu}$: 2958-2854 (alkyl C–H stretch); 1589 (C=N, pyridyl). *Anal. Calc. for* $C_{26}H_{28}N_6$: C, 73.56; H, 6.65; N, 19.79. *Found*: C, 73.22; H, 6.72; N, 19.72. MS-ES$^+$, *m*/*z*: 425.2194 (M + 1)$^+$; 447.2259 (M + Na)$^+$; 471.3126 (M + 2Na)$^+$.

(**L2**) Yield: 833 mg (64%). ^{1}H NMR (500 MHz, D_2O spiked with DCl) δ (ppm): 8.60(d, 4H); 8.38 (t, 4H); 7.94 (d, 4H); 7.82 (t, 4H), 4.20 (s, 8H), 2.50 (t, 4H); 1.71(m, 2H). ^{13}C NMR (125 MHz, D_2O spiked with DCl) δ (ppm): 23.0; 52.5; 55.0; 127.1; 128.0; 128.0; 145.0; 148.0; 154.0. IR (KBr, 4000-400 cm^{-1}) $\bar{\nu}$: 2958-2854 (alkyl C–H stretch); 1589 (C=N, pyridyl). *Anal. Calc. for* $C_{27}H_{30}N_6$: C, 73.94; H, 6.89; N, 19.17; *Found*: C, 74.08; H, 6.96; N, 19.17. MS-ES$^+$ *m*/*z*: 439.2453 (M + 1)$^+$; 461.2428 (M + Na)$^+$.

(**L3**) Yield: 1367 mg (67%). ^{1}H NMR (500 MHz, CD_3OD) δ (ppm): 8.41 (d, 4H); 7.77 (td, 4H); 7.58 (d, 4H); 7.26 (tt, 4H); 3.31 (m, 8H); 2.45 (s, br, 4H); 1.49 (m, 4H). IR (KBr, 4000-400 cm^{-1}) $\bar{\nu}$: 2958-2854 (alkyl C–H stretch); 1589 (C=N, pyridyl). *Anal. Calc. for* $C_{28}H_{32}N_6$: C, 74.30; H, 7.13; N, 18.57; *Found*: C, 74.30; H, 7.13; N, 18.53. MS-ES$^+$, *m*/*z*: 453.2199 (M + 1)$^+$; 475.2120 (M + Na)$^+$.

(**L4**) Yield: 604 mg (28%). ^{1}H NMR (500 MHz, D_2O) δ (ppm): 8.30 (d, 4H); 7.68 (t, 4H); 7.30 (d, 4H); 7.20 (t, 4H); 3.70 (s, br, 4H); 3.40 (m, 8H); 2.00 (s, 4H). IR (KBr, 4000-400 cm^{-1}) $\bar{\nu}$: 2958-2854 (alkyl C–H stretch); 1589 (C=N, pyridyl). *Anal. Calc. for*

$C_{30}H_{36}N_6$: C, 74.96; H, 7.55; N, 17.49; *Found*: C, 74.96; H, 7.52; N, 17.92. *m/z*: 481.9523 $(M + 1)^+$.

(**L5**) Yield: 996 mg (44%). ^{1}H NMR (500 MHz, D_2O spiked with DCl) δ (ppm): 8.50 (d, 4H); 8.26 (t, 4H); 7.82 (d, 4H); 7.70 (t, 4H), 4.15 (s, 8H), 2.45 (t, 4H); 1.20 (m, 4H); 0.85 (m, 8H). ^{13}C NMR (125 MHz, D_2O spiked with DCl) δ (ppm): 25.0; 26.2; 28.4; 54.8; 55.3; 127.1; 128.0; 142.0; 146.0; 154.2. IR (KBr, 4000-400 cm^{-1}) $\bar{\nu}$: 2958-2854 (alkyl C–H stretch); (C=N, pyridyl). *Anal. Calc. for* $C_{32}H_{40}N_6$: C, 75.56; H, 7.92; N, 16.52; *Found*: C, 75.80; H, 8.02; N, 16.73. MS-ES$^+$, *m/z*: 509.2449 $(M + 1)^+$; 510.2950 $(M + 2)^+$; 531.26.71 $(M + Na)^+$.

(**L6**) Yield: 859 mg (35%). ^{1}H NMR (500 MHz, D_2O spiked with DCl) δ (ppm): 8.49 (d, 4H); 8.26 (t, 4H); 7.82 (d, 4H); 7.70 (t, 4H), 4.15 (s, 8H), 2.45 (t, 4H); 1.20 (m, 4H); 0.85 (m, 12H). ^{13}C NMR (125 MHz, D_2O spiked with DCl) δ (ppm): 25.0; 26.2; 28.4; 28,5; 54.8; 55.5; 127.1; 128.0; 142.0; 146.0; 154.0. IR (KBr, 4000-400 cm^{-1}) $\bar{\nu}$: 2958-2854 (alkyl C–H stretch); 1589 (C=N, pyridyl). *Anal. Calc. for* $C_{34}H_{44}N_6$: C, 76.08; H, 8.26; N, 15.56; *Found*: C, 75.95; H, 8.33; N, 15.54.

Synthesis of complexes

The dinuclear Pt(II) complexes (**1** to **6**), and the mononuclear Pt(II) complex (**7**), listed below were synthesized starting from ligand **L1** to **L6** and *N*,*N*-bis(2-pyridylmethyl)amine, respectively, following a literature procedure reported by Hofmann *et al.*[14a]

[{Pt(Cl)}$_2$(*N*,*N*,*N*′,*N*′-tetrakis(2-pyridylmethyl)-1,2-ethanediamine)](ClO$_4$)$_2$ (**1**); [{Pt(Cl)}$_2$(*N*,*N*,*N*′,*N*′-tetrakis(2-pyridylmethyl)-1,3-propanediamine)](ClO$_4$)$_2$ (**2**); [{Pt(Cl)}$_2$(*N*,*N*,*N*′,*N*′-tetrakis(2-pyridylmethyl)-1,4-butanediamine)](ClO$_4$)$_2$ (**3**); [{Pt(Cl)}$_2$(*N*,*N*,*N*′,*N*′-tetrakis(2-pyridylmethyl)-1,6-hexanediamine)](ClO$_4$)$_2$ (**4**); [{Pt(Cl)}$_2$(*N*,*N*,*N*′,*N*′-tetrakis(2-pyridylmethyl)-1,8-octatanediamine)](ClO$_4$)$_2$ (**5**); [{Pt(Cl)}$_2$(*N*,*N*,*N*′,*N*′-tetrakis(2-pyridylmethyl)-1,10-decanediamine)](ClO$_4$)$_2$ (**6**) and [Pt(Cl)(*N*,*N*-bis(2-pyridylmethyl)amine)](ClO$_4$) (**7**).

Their purity was confirmed by ^{1}H NMR, ^{195}Pt NMR, micro analysis and infrared (IR). The IR spectra of all the complexes showed common characteristic peaks in the ranges 320-340 cm^{-1} (weak) and 1090-1100 cm^{-1} (broad, strong). These are due to Pt–Cl and Cl–O (perchlorate counter ion) vibrational stretches, respectively. The latter vibrational peaks confirm the cationic nature of the complexes.

(**1**) Yield: 153.6 mg (59%). ^{1}H NMR (500 MHz, DMF-d$_7$) δ (ppm): 8.78 (d, 4H); 8.33 (td, 4H); 7.77 (t, 8H); 7.72(d, 4H); 5.45 (d, 4H); 5.08 (d, 4H). ^{195}Pt NMR (107 MHz, DMF-d$_7$) δ (ppm): -2339.3. IR (KBr, 4000-300 cm^{-1}) $\bar{\nu}$: 2958-2854 (alkyl C–H stretch); 1589 (C=N, pyridyl); 1090-1100 (perchlorate counter ion); 324-330 Pt–Cl stretch). *Anal. Calc. for* $Pt_2C_{26}H_{28}N_6Cl_4O_8$: C, 28.79; H, 2.60; N, 7.75; *Found*: C, 28.73; H, 2.72; N, 7.90.

(**2**) Yield: 187.2 mg (71%). ^{1}H NMR (500 MHz, DMF-d$_7$) δ (ppm): 8.71 (dd, 4H); 8.35 (td, 4H); 7.76 (d, 8H); 5.40 (d, 4H); 4.98 (d, 4H); 3.20 (m, 4H); 2.30 (m, 4H). ^{195}Pt NMR (107 MHz, DMF-d$_7$) δ (ppm): -2344.8. IR (KBr, 4000-300 cm^{-1}) $\bar{\nu}$: 2958-2854 (alkyl C–H stretch); 1589 (C=N, pyridyl); 1090-1100 (perchlorate counter ion); 324-330 (Pt–Cl stretch). *Anal. Calc. for* $Pt_2C_{27}H_{30}N_6Cl_4O_8$: C, 29.51; H, 2.75; N, 7.65; *Found*: C, 29.12; H, 2.95; N, 7.48.

(**3**) Yield: 213.6 mg (81%). ^{1}H NMR (500 MHz, DMF-d$_7$) δ (ppm): 8.85 (d, 4H); 8.34 (td,4H);7.81 (d, 4H); 7.75 (t, 4H); 5.40 (d, 4H); 4.90 (d, 4H); 3.55 (s(br), 4H); 2.15 (s (br), 4H). ^{195}Pt NMR (107 MHz, DMF-d$_7$) δ (ppm): -2348.8. IR (KBr, 4000-300 cm^{-1}) $\bar{\nu}$: 2958-2854 (alkyl C–H stretch); 1589 C=N, (pyridyl); 1090-1100 (perchlorate counter ion); 324-330 Pt–Cl stretch). *Anal. Calc. for* $Pt_2C_{28}H_{30}N_6Cl_4O_8$: C, 30.22; H, 2.89; N, 7.55; *Found*: C, 30.38; H, 2.93; N, 7.50.

(**4**) Yield: 211.3 mg (77%). ^{1}H NMR (500 MHz, DMF-d$_7$) δ (ppm): 9.00 (d, 4H); 8.40 (td,4H);7.90 (d, 4H); 7.80 (t, 4H); 5.40 (d, 4H); 5.00 (d, 4H); 3.15 (s(br), 4H); 1.60 (s (br), 4H); 1.10 (s (br), 4H). ^{195}Pt NMR (107 MHz, DMF-d$_7$) δ (ppm): -2347.0. IR (KBr, 4000-300 cm^{-1}) $\bar{\nu}$: 2958-2854 (alkyl C–H stretch); 1589 C=N, (pyridyl); 1090-1100 (perchlorate counter ion); 324-330 (Pt–Cl stretch). *Anal. Calc. for* $Pt_2C_{30}H_{36}N_6Cl_4O_8$: C, 31.58; H, 3.18; N, 7.36; *Found*: C, 31.14; H, 3.11; N, 7.22.

(**5**) Yield: 230.0 mg (82%). ^{1}H NMR (500 MHz, DMF-d$_7$) δ (ppm): 9.05 (d, 4H); 8.40 (td,4H);7.92 (d, 4H); 7.80 (t, 4H); 5.45 (d, 4H); 5.12 (d, 4H); 3.20 (s(br), 4H); 1.60 (s (br), 4H); 1.10 (s (br), 8H). ^{195}Pt NMR (107 MHz, DMF-d$_7$) δ (ppm): -2345.6. IR (KBr, 4000-300 cm^{-1}) $\bar{\nu}$: 2958-2854 (alkyl C–H stretch); (1589 (C=N, pyridyl); 1090-1100 (perchlorate counter ion); 324-330 (Pt–Cl stretch). *Anal. Calc. for* $Pt_2C_{32}H_{40}N_6Cl_4O_8$: C, 32.88; H, 3.44; N, 7.19; *Found*: C, 32.41; H, 3.38; N, 7.22.

(**6**) Yield: 273 mg (95%). ^{1}H NMR (500 MHz, DMF-d$_7$) δ (ppm): 9.05 (d, 4H); 8.40 (td, 4H); 7.94 (d, 4H); 7.79 (t, 4H); 5.45 (d, 4H); 5.10 (d, 4H); 3.20 (s (br), 4H); 2.15 (s, 4H); 1.65 (s (br), 4H); 1.10 (s (br), 8H). ^{195}Pt NMR (107 MHz, DMF-d$_7$) δ (ppm): -2346.9. IR (KBr, 4000-300 cm^{-1}) $\bar{\nu}$: 2958-2854 (alkyl C–H stretch); 1589 (C=N, pyridyl); 1090-1100 (perchlorate counter ion); 324-330 (Pt–Cl stretch). *Anal. Calc. for* $Pt_2C_{34}H_{44}N_6Cl_4O_8$: C, 34.12; H, 3.70; N, 7.02; *Found*: C, 34.12; H, 3.79; N, 6.93.

(**7**) Yield: 228.4 mg (90%). ^{1}H NMR (400 MHz, DMF-d$_7$) δ (ppm): 9.05 (d, 2H); 8.50 (t, 2H); 8.05 (d, 2H); 7.79 (t, 2H); 5.3 (d,d, 2H); 5.10 (d,d 2H).^{13}C NMR (125 MHz, $CDCl_3$) δ (ppm): 60; 123.0; 126.0; 142.0; 149.0; 168. ^{195}Pt NMR (107 MHz, DMF-d$_7$) δ (ppm): -2340. IR (KBr, 4000-300 cm^{-1}) $\bar{\nu}$: 2958-2854 (alkyl C–H stretch); 1589 (C=N, pyridyl); 1090-1100 (perchlorate counter ion); 324-330 (Pt–Cl stretch). *Anal. Calc. for* $PtC_{12}H_{13}N_3Cl_2O_4$: C, 27.23; H, 2.48; N, 7.94; *Found*: C, 27.43; H, 2.52; N, 8.03.

Preparation of aqua complexes and nucleophile solutions

The kinetic solutions listed below were prepared following a literature procedure of Bugarčić *et al.*[22] [{Pt(H$_2$O)}$_2$(*N*,*N*,*N*′,*N*′-tetrakis(2-pyridylmethyl)-1,2-ethanediamine)](CF$_3$SO$_3$)$_4$, **En**; [{Pt(H$_2$O)}$_2$(*N*,*N*,*N*′,*N*′-tetrakis(2-pyridylmethyl)-1,3-propanediamine)](CF$_3$SO$_3$)$_4$, **Prop**; [{Pt(H$_2$O)}$_2$(*N*,*N*,*N*′,*N*′-tetrakis(2-pyridylmethyl)-1,4-butanediamine)](CF$_3$SO$_3$)$_4$, **But**; [{Pt(H$_2$O)}$_2$-(*N*,*N*,*N*′,*N*′-tetrakis(2-pyridylmethyl)-1,6-hexanediamine)](CF$_3$-SO$_3$)$_4$, **Hex**; [{Pt(H$_2$O)}$_2$(*N*,*N*,*N*′,*N*′-tetrakis(2-pyridylmethyl)-1,8-octatanediamine)](CF$_3$SO$_3$)$_4$, **Oct**; [{Pt(H$_2$O)}$_2$(*N*,*N*,*N*′,*N*′-tetrakis(2-pyridylmethyl)-1,10-decanediamine)](CF$_3$SO$_3$)$_4$, **Dec** and [Pt(H$_2$O)(*N*,*N*-bis(2-pyridylmethyl)amine)](CF$_3$SO$_3$)$_2$, **bpma**.

To a suspension of about 0.5 mmol of the [{Pt(Cl)}$_2$(*N*,*N*,*N*′,*N*′-tetrakis{(2-pyridylmethyl)-N(CH$_2$)$_n$N-](ClO$_4$)$_2$, n = 2, 3, 4, 6, 8 and 10, in a 50 ml solution of 0.001 M CF_3SO_3H was added $AgSO_3CF_3$ (1.99 mol. equivalents of the complex) dissolved in 0.01 M CF_3SO_3H (10 mL) and the mixture left to stir for 24 h at 50 °C in the dark. The silver chloride precipitate that

formed was removed by filtering the mixture through a 0.45 μm nylon membrane filter (Millipore) and the resultant filtrate was made up to the 100 mL volume mark with a 0.01 M CF_3SO_3H solution whose ionic strength had been adjusted to 0.02 M with $LiSO_3CF_3$. For the preparation of the **bpma** solution, the same procedure was followed using a 0.98 mol. equivalent of $AgSO_3CF_3$. Similarly, solutions of the nucleophiles, *viz*., thiourea (tu), *N*,*N*′-dimethylthiourea (dmtu), *N*,*N*,*N*′,*N*′-tetramethylthiourea (tmtu) and iodide (I^-) were prepared by dissolving known amounts of the nucleophiles in a 0.01 M CF_3SO_3H solution whose ionic strength had been adjusted to 0.02 M ($LiSO_3CF_3$).

Instrumentation and measurements

Either a Bruker Avance DPX 500 or DPX 400 NMR spectrometer was used to follow the reactions of **bpma-Cl**, **Prop-Cl** and **Dec-Cl** with tu as well as to confirm the identity and purity of both the ligands and complexes. The kinetic experiments were initiated by mixing the chloride derivatives of the respective complexes with two (**bpma-Cl**) or three equivalents (dinuclear complexes) in an NMR tube at 25 °C. Elementary compositions of the ligands and complexes were determined on a Carlo Erba Elemental Analyzer 1106. Infrared spectra of all the compounds were recorded in the range 4000-300 cm^{-1} on a Spectrum One FT-IR as KBr pellets. UV-visible spectra and kinetic measurements of slow reactions were recorded on a Cary 100 Bio UV-visible spectrophotometer with a cell compartment thermostated by a Varian Peltier temperature controller having an accuracy of ± 0.05 °C. The pH measurements were recorded on a Jenway 4330 pH meter with a combined Jenway glass microelectrode that had been calibrated with standard buffer solutions of pH 4.0, 7.0 and 10.0 (Merck). The KCl solution in the reference electrode was replaced with a 3 M NaCl electrolyte to prevent precipitation of $KClO_4$ during use.[20a,23] Kinetic measurements of fast reactions were monitored using an Applied Photophysics SX.18 MV (v4.33) stopped-flow reaction analyzer coupled to an online data acquisition system. The temperature of the instrument was controlled to within ± 0.1 °C.

Determination of pK_a values of complexes

All pH measurements were made separately outside the stock solution. Small vials were used for sampling out aliquots (3 ml) of the aqua complex. After pH measurements, the complex was discarded to avoid its *in situ* precipitation as a chloro-derivative. The solution was titrated with NaOH within the pH range of 2 – 9. An example of the spectral changes recorded during the titration is shown for **En** in Fig. 1. To avoid dilution effects due to addition of titrant, a large volume (250 mL) of metal complex was used for titration and small granules of crushed pellets were used within the pH range of 2-3. The NaOH solutions of decreasing concentrations were used in a manner that ensured that as many evenly distributed points were collected on the rising or falling sections of the titration curve. After each addition of titrant, the solution was stirred before its pH and respective spectrum were recorded. The sample aliquots from each absorbance measurement were returned back to the stock solution after use. On addition of solutions of decreasing concentrations of CF_3SO_3H as titrant, the reversibility of the titration reaction was observed with the baseline remaining intact.

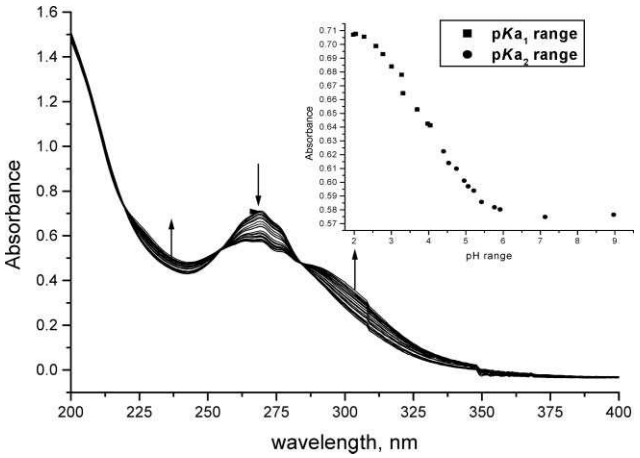

Fig. 1 UV-visible spectra for the titration of **En** (0.1 mM) with NaOH, pH range 2–9, $T = 298$ K. Inset is the titration curve at 268 nm.

Kinetic measurements

All substitution reactions were performed under pseudo first-order conditions. The nucleophiles were provided in concentrations of at least a 20-fold excess over that of the dinuclear Pt(II) complexes in all reactions. This afforded at least a 10-fold excess concentration of the nucleophiles at each Pt center which is considered sufficient to force the reactions to go to completion. Similarly for **bpma**, a 10-fold excess of concentration of nucleophiles over that of the metal complex was provided. A pH of 2.0 and an ionic strength of 0.02 M were maintained throughout the kinetic runs. All the wavelengths at which kinetic measurements were performed were predetermined spectrophotometrically by monitoring the change in absorbance of the mixture of the complex and the nucleophile as a function of time. These are summarized as ESI† in Table SI 1.

The temperature dependence of the observed rate constants for all reactions was studied over a temperature range of at least 20 °C. Kinetic measurements at elevated pressure (1–130 MPa) were performed on an in-house constructed high pressure stopped-flow instrument.[24] Only the first and faster reaction step involving reactions of all the dinuclear complexes with tu and tmtu nucleophiles was studied.

Computational details

Density functional theoretical (DFT)[25] calculations were performed with the Spartan '04 for Windows quantum chemical package[26] using the B3LYP,[27] a three parameter hybrid functional method, utilizing the LACVP+**[28] pseudo-potentials basis set. The dinuclear complexes and the monomeric **bpma** were all modeled as cations of a total charge of +4 and +2, respectively. In addition to the synthesized complexes, the calculations were extended to include two other dinuclear complexes bridged by alkyldiamine linkers with five- (**Pen**) and seven-CH_2 groups (**Hep**).

Results

Acid–base equilibria of the complexes

Fig. 1 shows a typical example of the spectral changes observed during the titration of the **En** complex with NaOH. All spectra

Table 1 Summary of pK_a data for the deprotonation of Pt-bound aqua ligands (within the pH range 2–9)[a]

	bpma	En	Prop	But	Hex	Oct	Dec
pK_{a1}	5.49 ± 0.08[b]	3.31 ± 0.19	3.95 ± 0.10	4.07 ± 0.05	4.64 ± 0.17	4.23 ± 0.15	4.53 ± 0.03
pK_{a2}		4.31 ± 0.29	6.30 ± 0.04	5.26 ± 0.06	5.68 ± 0.07	5.59 ± 0.18	

[a] The titration data for the complexes were fitted to equation, $y = a + (b - a)/(1 + 2.718\wedge((x - pK_{a1}/m) + (c - b)/(1 + 2.718\wedge((x - pK_{a2})/n))$, for measuring two p$K_a$ values or the Boltzmann equation, $y = A_2 + (A_1 - A_2)/(1 + \exp((x - x_0)/dx)$, for measuring one p$K_a$ value using the Origin 7.5® program. [b] Data quoted from Ref. 30.

recorded in each titration passes through three isosbestic points (see also Figure SI 1, ESI,† for **Oct**). The pK_a values for the complexes were determined from the titration traces taken at specific wavelengths from their repetitive spectra acquired during the pH changes. A representative spectral plot is shown as an inset in Fig. 1.

The data was fitted to a standard equation for measuring two pK_a values using the Origin 7.5®[29] software. The titration data for all dinuclear complexes except for **Dec** fitted better to the equation describing two pK_a values. The data obtained including the value for **bpma**[30] is presented in Table 1.

Data in Table 1 shows that when the pK_a value of **bpma** is taken as the reference, the first pK_a values of all the dinuclear complexes are at least one pH unit lower than that of **bpma**. While the first pK_a values for complexes with longer bridges, *viz*., **Hex**, **Oct** and **Dec** are statistically constant, it is noted that the first pK_a values increases proportionally from 3.31 to 4.64 as the chain length of the linker is increased from **En** to **Hex** with the exception of **Prop**. It is also noted that the deprotonation of the second aqua ligand to form the hydroxo/hydroxo species occurs at higher pH values than that of the first.

Computational calculations

In order to gain an in-depth understanding of the structural as well as the electronic differences that exist in the complexes under study, we performed computational calculations and representative geometry-optimized structure for the **bpma**; **En**; **Prop** and **Dec** complexes and an extract of the calculated data is presented in Tables 2 and 3, respectively.

The minimum energy structures of the included odd-bridged complexes (**Pen** and **Hep**) are provided as ESI† in Table SI 5. The model structures in Table 2 reveals that when the number of CH_2 groups in the linker is even, the structures adopt the C_{2h} point group symmetry, whereas a C_{2v} symmetry is preferred for **Prop** and its two other analogues with an odd number of carbon atoms in the diamine bridge (**Pen** and **Hep**, Table SI 5, ESI†). The pertinent angles to the structural metrics of the complexes are depicted in Fig. 2 for **En**; **Prop** and **Dec**.

The geometry about the Pt atoms is slightly distorted square-planar.[31a] The coordinated aqua ligands in **En** are 19.5° out of plane, while the aqua ligand in the **bpma** complex is tilted by only 10.69°, a value which compares well to a measured value of 10.51° for [Pt(*N*,*N*-bis(2-pyridylmethyl)amine)(H_2O)]ClO_4·$2H_2O$, retrieved from the Cambridge Crystallographic database.[31b] However, on extending the length of the linker to **Dec** the angling decreases to 14.85°. Due to some moderate flexibility introduced by the methylene carbons of the picolyl units in the chelate framework, overcrowding around the Pt atom is averted by assuming an out-tipped conformation of the tertiary nitrogen atoms relative to the plane containing the atoms of Pt and picolyl units. This causes the angling down of the terminal aqua ligands. The increase in the angling out of the aqua ligands of all the dinuclear complexes when compared to **bpma**, is a clear sign that the PtN_3 coordination plane is under steric strain on one of its sides, which originate from the bridging linker. The magnitude of this strain depends on the angle of inclination, α, as well as the length of the linker, decreasing from the vertically inclined shorter linker in **En** (74.2°) to the less inclined linker of **Dec** (44.6°). These inclination angles are referenced to the mean plane containing the Pt(II) atom and the atoms of the picolyl units as illustrated in the DFT calculated structures of **En** and **Dec** in Fig. 2.

A similar angle for the complexes with odd numbers of CH_2 groups in the linker (**Prop**, **Pen**, and **Hep**) could not be determined because of the shape of the structures they adopted.

The mappings of the frontier orbitals (Table 2) are similar for all the complexes. The HOMO orbitals are concentrated on the pyridyl π-acceptor carrier ligands and shared with the Pt(II) metal ions. However, the LUMO is centred primarily on the metal center and the donor atoms of the chelating ligands. Both frontier orbitals have no electron density mapping within the linker piece. The similarity in the locations of the HOMO orbitals in these complexes is consistent with an effective π-back donation of electron density from the metal center into the two pyridyl units of the chelate due to their strong π-acceptability.[20] However, a general increase in the energy gap, $\Delta E_{(HOMO-LUMO)}$, of the frontier orbitals is observed as the chain length is increased. It is also noted that the Pt atoms in all dinuclear complexes carry symmetrical non-bonding orbital (NBO) charges suggesting that the metal centers are in the same electronic environment. However, the variation of the calculated charges with chain length is not linear as would be predicted on the basis of σ-inductive effects due to the linker towards the Pt atoms.

Kinetics

The substitution of the aqua ligands in dinuclear Pt(II) complexes with bis(2-pyridylmethyl)amine chelates and in the monomeric analogue, **bpma**, by the thiourea nucleophiles and iodide occurs through two well separated steps, *viz*., the simultaneous substitution of the coordinated aqua ligands and the dechelation of the *cis*-pyridyl ligands, as reported in previous studies[14a-c] for the former complexes.

Two observations stimulated this generalization. Firstly, we noticed that the substitution of the coordinated aqua ligands in **Dec** can be fitted to two separate exponential functions despite the deprotonation equilibria showing a single pK_a value. This anomaly had been observed before,[14b] where the substitution of aqua ligands

Table 2 Density functional theoretical (DFT)[25] minimum energy structures, HOMO and LUMO frontier molecular orbitals for **bpma**, **En**, **Prop** and **Dec**. The calculations were performed with the Spartan '04 for Windows quantum chemical package[26] using the B3LYP hybrid functional method[27] utilizing the LACVP+**[28] pseudo-potentials basis set

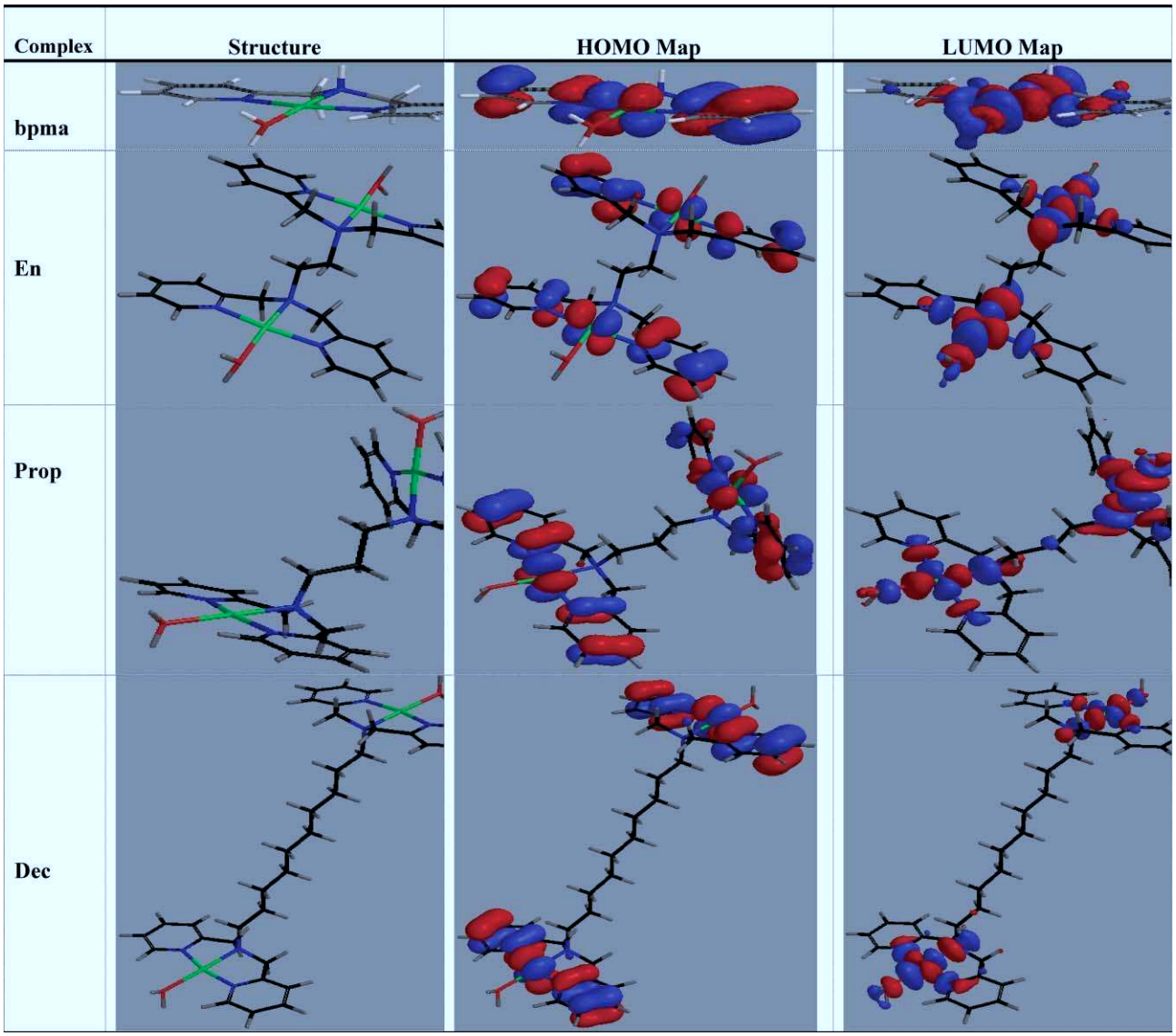

in **Dec** by a chloride anion could be fitted both to a single as well as a double exponential fit. However, using ^{195}Pt NMR and thiourea as the nucleophile, clear cut evidence of dechelation of the pyridyl units was confirmed,[14c] suggesting that the substitution of the coordinated aqua ligands on the Pt metal centers in **Dec**, occurs simultaneously. Thus, the second step observed in the former studies[14b,c] and confirmed in this study for this complex, can only be reasonably ascribed to the dechelation of one of the coordinated pyridyl ligands by the incoming nucleophiles.

Secondly, we observed the existence of a second substitution step in monomeric **bpma** by the thiourea nucleophiles which slowly reaches equilibrium. A representative of the time-resolved kinetic trace showing the two separate substitution steps is shown in Figure SI 2a (ESI†) for the reaction between **bpma** (0.1 mM) and tu (3 mM). In all reported ligand substitution reactions for this complex using sulfur containing nucleophiles[20,23,30,32a,33] as well as anionic sulfur nucleophiles[14a,32b,33] as entering groups, nothing was mentioned about this second and slower substitution step. Thus, these two anomalous observations are in line with a mechanism consistent with ring opening as the second and slower observed step in both the **bpma** and **Dec** complexes.

To further confirm this, we studied the substitution reactions of three of the complexes, *viz*., **bpma-Cl**, **Prop-Cl** and **Dec-Cl**, using ^{1}H NMR spectroscopy. An array of the ^{1}H NMR spectra (showing only the aromatic resonances) for the reaction between **bpma-Cl** and two equivalents of tu (in DMF-*d*7) is shown in Fig. 3.

In all experiments involving the three complexes, a new set of resonances shifted downfield and integrating to an approximate ratio of to 2 : 1 (intermediate product : reactant) upon mixing the complexes with at least two equivalents of thiourea is observed for the H_5/H_5, protons on the pyridine rings. The adopted numbering system for the pyridyl protons used to monitor the progress of

Table 3 Summary of the calculated structural data at the DFT[25] level of theory for the complexes with bis(2-pyridylmethyl)amine chelates

Complex	bpma	En	Prop	But	Pen	Hex	Hep	Oct	Dec
Property									
Bond lengths, Å									
Pt-OH_2 Pt–N_{trans}	2.151 2.012	2.140 2.052	2.141 2.057	2.143 2.054	2.149 2.049	2.149 2.049	1.214 2.043	2.155 2.045	2.157 2.042
Separation distance, Å									
$Pt_{1\ coord.\ plane} - Pt_{2\ coord.\ plane}$[i]		3.63		4.28		5.84		7.39	9.16
Bond angles, °									
N_{cis}-Pt–N_{cis}	165.75	166.31	167.03	167.07	166.93	166.95	166.81	166.95	166.73
Pt_1–$N_{1\ trans}$–$N_{2\ trans}$		105.80	137.85	134.50	142.9	135.76	148.4	136.51	135.37
β			124.0		139.8		160.8		44.57
Elevation angle of bridge, α[a]		74.20		45.50		44.24		43.49	
Inclination angle of aqua ligands	10.69	19.50	14.85	16.74	13.85	16.11	13.37	15.36	14.85
Energy gap, eV									
$\Delta E_{LUMO\text{-}HOMO}$,	5.23	5.00	4.99	5.07	5.12	5.14	5.18	5.18	5.19
Natural charges									
$Pt_{(1/2)}$	1.218	1.220	1.223	1.222	1.218	1.217	1.214	1.213	1.211
Point group symmetry of the complexes	C_{2v}	C_{2h}	C_{2v}	C_{2h}	C_{2v}	C_{2h}	C_{2v}	C_{2h}	C_{2h}

[a] α is the supplementary angle to the angle {Pt1-N1$_{trans}$-N2$_{trans}$} in complexes with C_{2h} symmetry. The projected separation distance between the first coordination plane and the second ($Pt_{1\ coord.\ plane} - Pt_{2\ coord.\ plane}$)[i] was calculated using α and the length of the linker ($N_{1\ trans} - N_{2\ trans}$) as depicted in structures of **En** and **Dec** in Fig. 2 while the angle β, subtended by the overlooking faces of the chelate was estimated as illustrated for the structure of **Prop** in the same Figure.

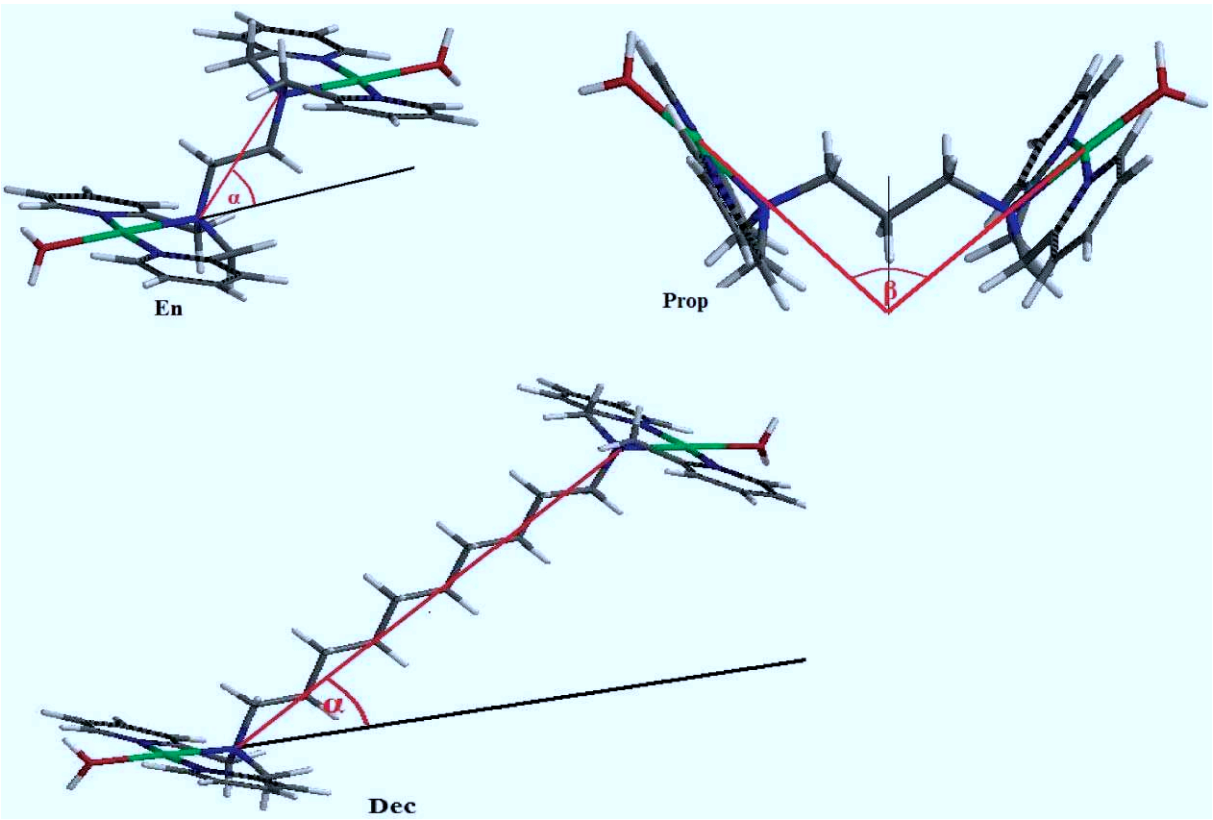

Fig. 2 Aerial view showing the angles of inclination, α, in the DFT calculated slip-up sandwich structures of **En** and **Dec** and the hinge angle, β, in the bowl structure of **Prop**.

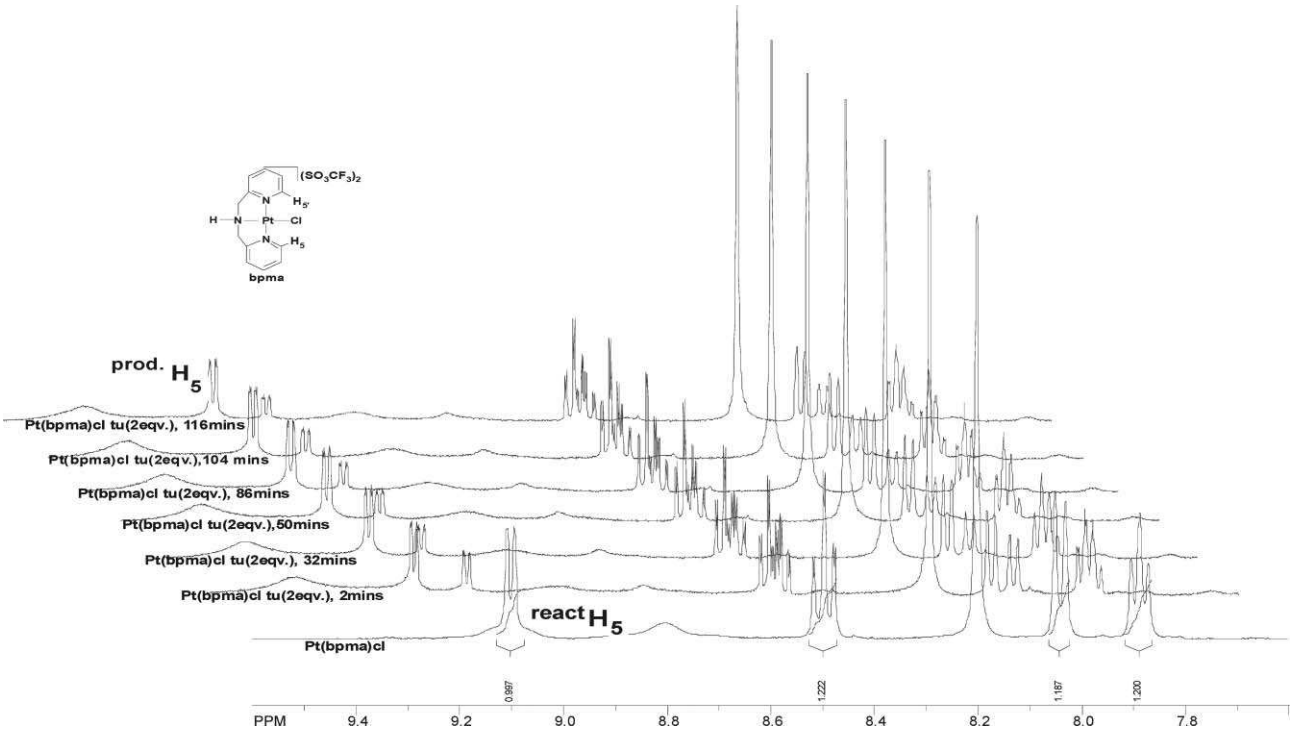

Fig. 3 ^{1}H NMR (500 MHz) spectra array of **bpma-Cl** (the aromatic region) acquired during its reaction with two equivalents of thiourea (tu) in DMF-*d*7 at 298 K. The doublet at $\delta = 9.12$ ppm corresponds to the substituted product.

the reaction is shown in the structure of the **bpma Cl** complex as an inset in Fig. 3. A distinctive shift in the chemical shift of the H_5 protons relative to the other three ring protons upon coordination of tu at the metal center is due to their close proximity to the N donor atom of the rings. As a result and can be noted in the spectral arrays of the reaction of **bpma**, the electronic environments of the other pyridyl protons are not affected to a great extent by the coordination of thiourea. Thus, the H_5 resonances were chosen to monitor the kinetic progression of the reaction.

The H_5 resonances of the **bpma-Cl** complex, labeled $^{react.}H_5$, which appear at $\delta = 9.06$ ppm are shifted downfield to $\delta = 9.12$ ppm in the tu-substituted derivative, labeled $^{prod.}H_5$ in Fig. 3. During the reaction, the $^{prod.}H_5$ resonances of the intermediate product formed on the onset further grew while $^{react.}H_5$ decreased accordingly. Since the first step which involves the substitution of the chloride ligands is fast and complete in less than 20 s for all these complexes, it cannot be monitored by the NMR technique due to the limitations in the slow manual mixing of the reactants. Thus, it can be assumed that the subsequent changes in the arrays are certainly due to another step which is evidently observed in **bpma-Cl** as well, a mononuclear analogue with one leaving group. From the spectral arrays of the other complexes, again only two sets of H_5 resonances are observed upon mixing the dinuclear complexes with three equivalents of tu. No extra sets of resonances, in support of a stepwise second substitution were observed during the progression of the reactions with tu for up to three hours. In principle, the spectral arrays of **Prop-Cl** and **Dec-Cl** show the same pattern of substitution as observed in **bpma-Cl**. The spectral array for the reaction between **Dec-Cl** and three equivalents of tu is presented in Figure SI 2b (ESI†).

If all the facts are added together, they clearly reiterate that the substitution of the chloride or aqua ligands in the dinuclear complexes occurs simultaneously irrespective of the length of the linker or the symmetry of the complexes. Based on the NMR study of **bpma-Cl**, it is reasonable to conclude that the ring opening is endemic to the bis(2-pyridylmethyl)amine carrier ligand core despite the carrier ligand forming five-membered chelated rings which are known to be thermodynamically stable.[34] It is unlikely that the chain length of the diamine linker and hence the average distance separating the Pt centers causes this. It can therefore be assumed that the second and slower subsequent steps as observed in all the other dinuclear complexes bearing this carrier ligand as well as **bpma** are in fact the dechelation of the pyridyl units. The general reaction pathway for the substitution of the coordinated aqua ligands and the induced ring opening of the chelate ligand by the strong labilizing thiourea nucleophiles can therefore be represented by Figure SI 2c (ESI†). Another observation in support of this is the second substitution step of all the reactions which is invariably 100 times slower when compared to the first. Relative to the first step, the rate constants for the second step depend weakly on the variation in the length of the alkanediamine linkers.

The two substitution steps were followed separately on the stopped-flow reaction analyzer. The first step is fast and complete within 50 s. The second substitution step for the reactions between all nucleophiles and the least reactive complexes, *viz*., **En** and **But**, were also repeated using UV-visible spectroscopy and followed for more than four half-lives of the second and slower substitution step to offer a comparison with the results from the stopped-flow analyzer. An example of a kinetic trace recorded on a UV-visible spectrophotometer for the analysis of the dechelation and slower

substitution step for the reaction between **En** (0.1 mM) and tu (6 mM) at 298 K, pH = 2.0, I = 0.02 M {CF_3SO_3H, adjusted with $Li(SO_3CF_3)$} is shown in Fig. 4.

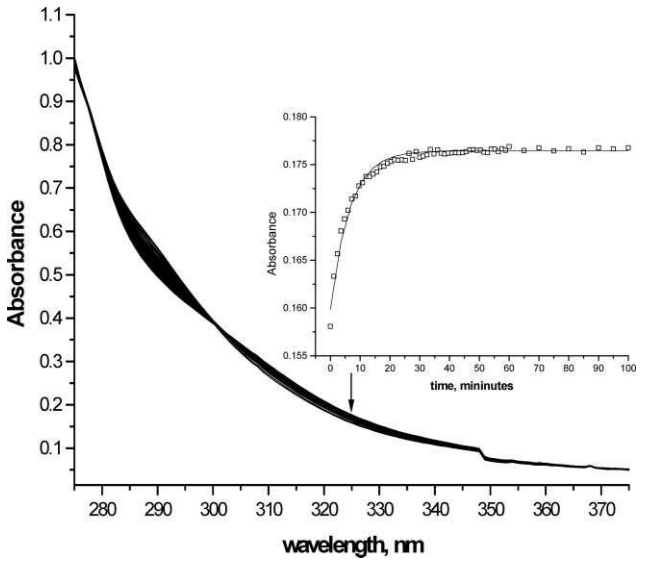

Fig. 4 A typical plot of the changes in absorbance observed within the 275-400 nm avelength range for the dechelation of the pyridyl units in **En** (0.1 mM) by tu (6 mM) at 298 K, pH = 2.0, I = 0.02 M {CF_3SO_3H, adjusted with $Li(SO_3CF_3)$}. Inset: Kinetic trace taken at 325 nm.

The pseudo first-order rate constants, $k_{obs(1^{st}/2^{nd})}$, calculated from such kinetic traces were plotted against the concentration of the entering nucleophiles using the Origin 7.5®[29] software. Examples of plots of the observed pseudo first-order rate constants, $k_{obs(1^{st}/2^{nd})}$, against concentration of the nucleophiles for the two reaction steps is shown in Fig. 5a and 5b for **En**.

The slopes of the plots gave the second order rate constants $k_{2(1^{st}/2^{nd})}$, and their values are summarized in Table 4 for all the studied complexes.

Both substitution steps for all the complexes with the exception of **bpma** gave excellent linear fits passing through the origin indicating that the backward reactions are insignificant or absent. Thus, the mechanism of the substitution of the aqua ligands by the thiourea nucleophiles in these dinuclear complexes for both steps is as proposed in an earlier study by van Eldik and co-workers,[14c] and can thus be represented by Figure SI 2c (ESI†). The rate law can be expressed as in eqn (1).

$$k_{obs(1^{st}/2^{nd})} = k_{2(1^{st}/2^{nd})}[Nu] \quad (1)$$

The dechelation substitution step in **bpma**, however, gave a slight intercept when the observed first-order rate constant, $k_{obs(2^{nd})}$, was plotted against the concentration of the entering nucleophiles. Re-chelation of the pyridyl units at a pH of 2.0 can be ruled out since the N atoms of the pyridyl unit are protonated.[14c] The intercept is likely to be the slow aquation of the *cis*-coordinated thioureas which is assisted by steric repulsions from the dangling ends of the picolyl units.

A general look at the results in Table 4 shows that the simultaneous displacement of the aqua ligands as well as the subsequent dechelation of the pyridyl units is enhanced on increasing the chain length from **En** to **Dec**. An exception is **Prop**,

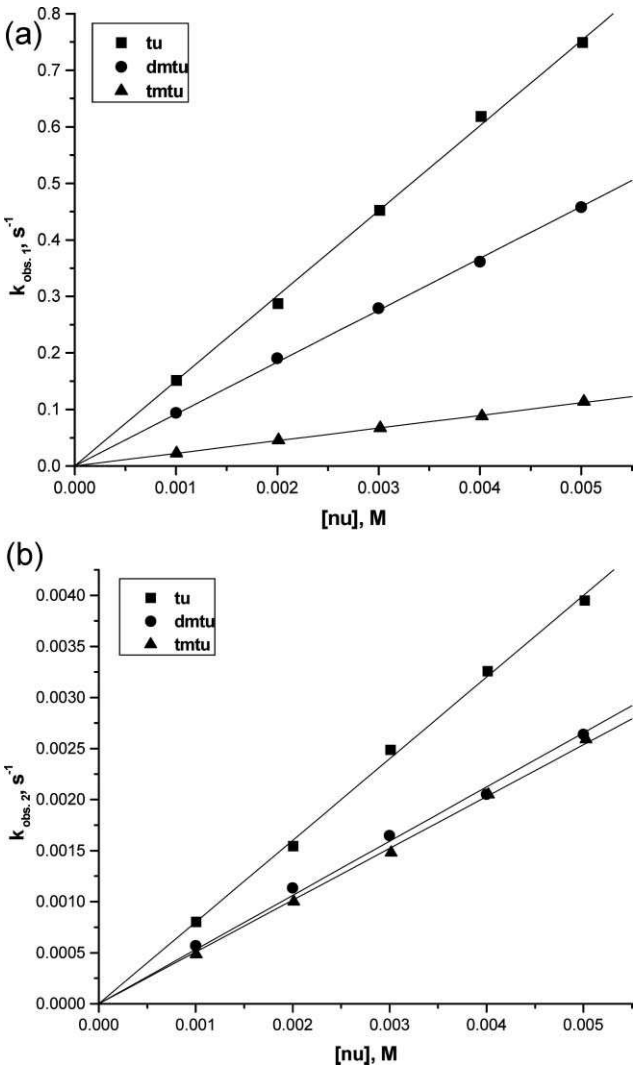

Fig. 5 (**a**) Concentration dependence of $k_{obs(1^{st})}$, s^{-1}, for the simultaneous displacement of the aqua ligands in **En** by thiourea nucleophiles, pH = 2.0, T = 298 K, I = 0.02 M {0.01 M CF_3SO_3H, adjusted with $Li(SO_3CF_3)$}. (**b**) Concentration dependence of $k_{obs(2^{nd})}$, s^{-1}, for the dechelation of the pyridyl units in **En** by thiourea nucleophiles, pH = 2.0, T = 298 K, I = 0.02 M {0.01 M CF_3SO_3H, adjusted with $Li(SO_3CF_3)$}.

which shows unusual high reactivity towards all the nucleophiles surpassing even **Dec**. This increase in the rate of substitution is, however, marginal for the dechelation step. The other trend that is general across all the complexes is that the substitution of the aqua ligands is about 100 times faster than the dechelation of the picolyl units as already stated. A detailed analysis of the substitution of the coordinated aqua ligands by these nucleophiles in the complexes reveals that the order of substitutional reactivity is **En** < **But** < **bpma** < **Hex** ≈ **Oct** ≈ **Dec** < **Prop**. Using **En**'s rate constant as the common value, the ratios of the rate of substitution of the aqua ligands of **En**, **But**, **Hex**, **Oct** and **Dec** by tu is 1: 2.1: 3.8: 3.8: 4.2, respectively. Thus, on extending the chain length of the bridge beyond **Hex**, the reactivity does not change significantly. The leveling effect of the reactivity and hence the similarity in the kinetic behaviour of the dinuclear complexes which are linked by flexible bridges of longer chain lengths (n = 8; 10) has been reported[14d] in a related study involving

Table 4 Summary of the second-order rate constants for the simultaneous displacement of aqua ligands and the dechelation of the pyridyl units by thiourea nucleophiles in **bpma** and a range of dinuclear complexes with bis(2-pyridylmethyl)amine chelate headgroups

		Second order rate constant, M^{-1} s^{-1}	
Complexes	nu	$k_{2/1}{}^{st}$	$k_{2/2}{}^{nd}$
bpma	tu	409 ± 2	4.95 ± 0.06 $(3.9 \pm 1) \times 10^{-4}$ [a]
	dmtu	394 ± 1	4.05 ± 0.07 $(1.7 \pm 1) \times 10^{-4}$ [a]
	tmtu	190 ± 0.5	2.16 ± 0.06 $(3.3 \pm 1) \times 10^{-4}$ [a]
En	tu	151 ± 1	0.81 ± 0.02
	dmtu	92 ± 1	0.53 ± 0.01
	tmtu	23 ± 1	0.51 ± 0.01
	I^-	$(7.9 \pm 0.1) \times 10^3$	$(0.7 \pm 0.02) \times 10^3$
Prop	tu	1033 ± 7	4.53 ± 0.07
	dmtu	727 ± 3	4.78 ± 0.10
	tmtu	305 ± 2	3.13 ± 0.05
	I^-	$(29.1 \pm 0.8) \times 10^3$	$(6.6 \pm 0.2) \times 10^3$
But	tu	315 ± 1	1.16 ± 0.01
	dmtu	346 ± 2	1.04 ± 0.01
	tmtu	130 ± 1	0.50 ± 0.01
	I^-	$(14.1 \pm 0.7) \times 10^3$	$(4.5 \pm 0.1) \times 10^3$
Hex	tu	579 ± 2	5.30 ± 0.03
	dmtu	606 ± 4	5.86 ± 0.07
	tmtu	182 ± 1	1.23 ± 0.01
	I^-	$(11.4 \pm 0.3) \times 10^3$	$(5.8 \pm 0.2) \times 10^3$
Oct	tu	572 ± 3	6.24 ± 0.04
	dmtu	539 ± 5	5.38 ± 0.05
	tmtu	206 ± 2	2.76 ± 0.02
Dec	tu	641 ± 3	6.49 ± 0.15
	dmtu	632 ± 5	2.49 ± 0.02
	tmtu	198 ± 2	1.83 ± 0.01

[a] Value of k_{-2} for the back reaction step.

two *cis*-bridged dinuclear Pt(II) bearing [Pt(DACH), DACH = (1*R*,2*R*)-(−)-1,2-diaminocyclohexane] non-labile chelate ligands.

However, on changing the structural nature of the incoming nucleophile from tu to tmtu, the trend remains almost the same, but the reactivity gradient along the series is markedly lower than that of tu or dmtu. It is also noted that the rate of substitution of the aqua ligand of **bpma** by tmtu is comparable to that of the dinuclear complexes of longer chain length (**Hex**, **Oct** and **Dec**). This is despite an increase in σ-inductive donation[14d] towards each of their Pt atoms and a higher charge of +4. This poor sensitivity toward changes in the electronic properties along the series by the bulky tmtu nucleophile is indicative of the presence of steric effects along the series of complexes.

Results in Table 4 further reveals that the rates of the simultaneous displacement of the aqua ligands in the **En** and **But** complexes are in fact lower than that in **bpma**. For example, despite an increase in the overall charge of +4 in **En**, the **bpma** complex reacts faster by factors of about 2.7 (tu), 4.3 (dmtu) and 8.3 (tmtu) than the former.

The order of reactivity of the thiourea nucleophiles at the Pt centers increases in the order tu ≈ dmtu > tmtu and is in line with steric retardation in the case of tmtu and a dominating positive inductive effect in the case of dmtu. To test the reactivity trend observed for these complexes with the neutral nucleophiles, an ionic nucleophile (I^-) was also used. Plots demonstrating a linear dependence of the rate constant on both the iodide concentration and the temperature are given as supporting information, Figures SI 3e and 3f, respectively. The calculated kinetic data from these plots is presented in Tables 4 and 5. The order of reactivity for the complexes with the iodide (**En** < **But** ≈ **Hex** < **Prop**) remain similar to that already observed for the neutral thiourea nucleophiles.

Table 5 Summary of the activation parameters for the simultaneous displacement of aqua ligands and the dechelation of the pyridyl units by thiourea nucleophiles in **bpma** and a range of dinuclear Pt(II) complexes with bis(2-pyridylmethyl)amine chelate headgroups (— not determined)

		Activation enthalpy kJ mol^{-1}		Activation entropy J mol^{-1} K^{-1}		Activation volume cm^3 mol^{-1}
Complexes	**nu**	$\Delta H^{\neq}{}_1$	$\Delta H^{\neq}{}_2$	$\Delta S^{\neq}{}_1$	$\Delta S^{\neq}{}_2$	$\Delta V^{\neq}{}_1$
bpma	**tu**	41.1 ± 0.9	46.1 ± 0.3	−57 ± 3	−79 ± 1	—
	dmtu	37.2 ± 0.9	52.0 ± 1.2	−71 ± 3	−59 ± 4	—
	tmtu	43.3 ± 1.1	59.3 ± 1.0	−57 ± 3	−37 ± 3	—
En	**tu**	40.9 ± 1.2	25.5 ± 0.7	−66 ± 4	−157 ± 2	−4.0 ± 0.2
	dmtu	48.8 ± 2.0	36.0 ± 1.1	−64 ± 6	−130 ± 4	—
	tmtu	43.3 ± 1.2	53.4 ± 1.5	−105 ± 4	−76 ± 4	−4.6 ± 0.2
	I^-	45.0 ± 1.0	38.4 ± 1.3	−21 ± 3	−50 ± 4	—
Prop	**tu**	24.3 ± 0.7	20.7 ± 0.5	−106 ± 2	−161 ± 2	−5.5 ± 0.3
	dmtu	34.3 ± 0.7	27.5 ± 0.6	−75 ± 2	−137 ± 2	—
	tmtu	39.4 ± 0.4	41.1 ± 2.0	−64 ± 1	−97 ± 6	−13.2 ± 0.2
	I^-	24.7 ± 0.7	29.8 ± 0.8	−71 ± 2	−65 ± 3	—
But	**tu**	37.0 ± 0.8	32.5 ± 1.0	−73 ± 3	−135 ± 3	−4.0 ± 0.2
	dmtu	40.4 ± 1.0	29.7 ± 0.5	−61 ± 3	−161 ± 2	—
	tmtu	41.6 ± 0.7	42.4 ± 1.0	−65 ± 2	−153 ± 3	−8.9 ± 0.3
	I^-	17.5 ± 0.4	28.5 ± 0.2	−108 ± 1	−81 ± 1	—
Hex	**tu**	34.3 ± 0.7	38.9 ± 1.0	−77 ± 2	−101 ± 3	−3.1 ± 0.1
	dmtu	43.0 ± 1.0	42.5 ± 2.0	−47 ± 3	−88 ± 6	—
	tmtu	47.2 ± 0.6	27.2 ± 0.6	−42 ± 2	−147 ± 2	−9.3 ± 0.2
	I^-	25.7 ± 0.7	15.8 ± 0.7	−81 ± 2	−122 ± 2	—
Oct	**tu**	30.5 ± 0.6	24.5 ± 0.5	−90 ± 2	−148 ± 2	−4.7 ± 0.1
	dmtu	32.2 ± 0.3	27.5 ± 0.6	−84 ± 1	−138 ± 2	—
	tmtu	46.7 ± 0.1	48.2 ± 0.9	−46 ± 3	−80 ± 3	−8.5 ± 0.2
Dec	**tu**	34.0 ± 0.8	28.9 ± 1.1	−78 ± 2	−122 ± 3	−4.6 ± 0.1
	dmtu	36.7 ± 1.0	32.5 ± 1.2	−69 ± 3	−127 ± 4	—
	tmtu	53.6 ± 1.0	36.9 ± 0.9	−42 ± 3	−114 ± 3	−12.7 ± 0.4

Again, we notice the 'entrapment effect' of the **Prop** complex, a structural phenomenon which as already explained, leads to its exceptional higher reactivity with the anionic iodide nucleophile.

The dependence of the two observed pseudo first-order rate constants, $k_{obs(1^{st}/2^{nd})}$, on temperature and pressure (for the first substitution step with tu and tmtu) resulted in the activation parameters ($\Delta H^{\neq}_{(1^{st}/2^{nd})}$, $\Delta S^{\neq}_{(1^{st}/2^{nd})}$) and $\Delta V^{\neq}_{(1^{st})}$, respectively. Typical Eyring plots for the two steps are shown in Fig. 6a and 6b, respectively and the resultant activation enthalpy and entropy activation values are summarized in Table 5.

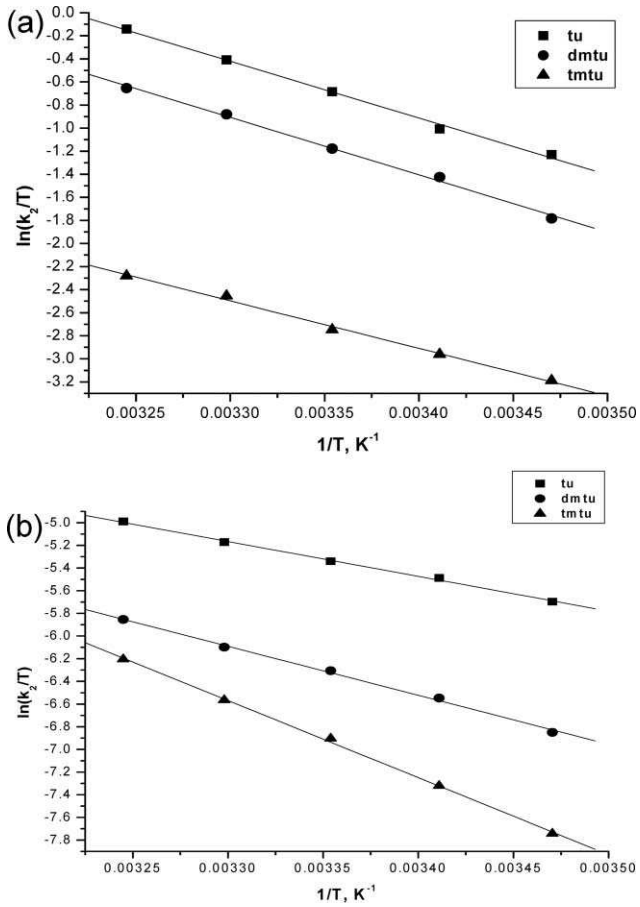

Fig. 6 (**a**) Temperature dependence of $k_{2(1^{st})}$, M^{-1} s^{-1}, for the simultaneous displacement of the aqua ligand in **En** by thiourea nucleophiles, pH = 2.0, I = 0.02 M {0.01 M CF_3SO_3H, adjusted with $Li(SO_3CF_3)$}. (**b**) Temperature dependence of $k_{2(2^{nd})}$, M^{-1} s^{-1}, for the dechelation of the pyridyl units of **En** by thiourea nucleophiles, pH = 2.0, I = 0.02 M {0.01 M CF_3SO_3H, adjusted with $Li(SO_3CF_3)$}.

Exemplary pressure dependence plots are provided for the reactions between **Prop** and **Oct** with tu in Figures SI 4a and 4b (ESI†), respectively and the calculated values of $\Delta V^{\neq}_{(1^{st})}$ are also presented in Table 5.

Discussion

Hydrolysis of complexes

The general increase in the basicity of the complexes as the length of the linker is increased is the result of an increase in the σ-induction[14d] to the Pt center due to the linker. This results in a decrease in the positive charge on the Pt atoms. This deduction is supported by the shortening of the Pt–N bond lengths as the length of the linker increases as shown in Table 3 and is reflected on the calculated NBO charges. The static ground effect of this is to weaken the Pt–O bond of the coordinated aqua through the *trans* influence, leading to an increase in basicity as the chain length is increased. This is supported by the Pt-OH_2 bond lengths which increase with increasing chain length of the linker (Table 3). Thus, the length of the alkyldiamine linker reduces the charge addition between the two Pt centers and increases the σ-inductive effects,[14d] two factors that control the net effective charge carried by the Pt centers. In the case of the **Dec** complex, the charge addition to each Pt center is almost absent such that each center can be assumed to act independently. It can therefore be concluded that in this series of dinuclear complexes, the acidity of the coordinated aqua ligand is in fact controlled by the effective charge on the Pt atoms, which depends on the length of the linker to some point.

The higher pH values recorded for the deprotonation of the second aqua ligand to form the hydroxo/hydroxo species indicates a general reduction in the overall charge on the first Pt atom on forming the hydroxo species.[14a] Like in the first deprotonation step, both effects depend on the chain length of the bridge up to a point. What is noted is that the pK_{a2} values for the deprotonation of the second coordinated aqua ligands in **Hex**, **Oct** and **Dec** approximate that of **bpma**. The observation that these three complexes have approximately equal pK_{a2} values is similar to the trend observed in their pK_{a1} values, signifying that the effect of the chain length has a limit, after which it has no influence on the net effective charge of the Pt centers. The overall deprotonation of the coordinated aqua ligands clearly follows a two-step process. Despite this, and as shall be discussed later, the substitution of the coordinated ligands by the thiourea nucleophiles is however not stepwise and does not follow the trend of the deprotonation of the coordinated aqua ligands.

Kinetics

An analysis of the rate constants for the simultaneous displacement of the coordinated aqua ligands by the thiourea nucleophiles shows that the symmetry architectures of the alkanediamine linker control the substitution process. We previously reported[35] on the crystal structures of two of the metal-free analogues of these metal complexes, *viz*., the ligands bridged by 1,3-propanediamine and 1,4-butanediamine chains. The number of CH_2 groups within the linker was found to play a pivotal role in the overall symmetry adopted by the ligands and also in their supramolecular chemistry. Thus, a crystallographic inversion symmetry of the metal-free ligands bearing an even number of CH_2 groups, confers a C_{2h} symmetry to the complexes upon their coordination to Pt(II) atoms, while a two-fold rotational symmetry of the free ligands bridged by linkers with an odd number of CH_2 groups as exemplified by the structures of **Prop**; **Pen** and **Hep** favors formation of dinuclear complexes with a C_{2v} symmetry (Tables 2 and SI 5). A consequent of this coordination requirement along the two square-planar chelates is to place the two Pt(II) centers into highly symmetrical environments upon their coordination to the bis(2-pyridylmethyl)amine chelates such that they can not be differentiated by the highly reactive sulfur nucleophiles. This symmetrical environment on the planes of the Pt atoms

is supported by the calculated NBO charges on the Pt atoms (Table 3) which reveal a symmetrical charge distribution on the Pt atoms in all the dinuclear complexes. A result is the simultaneous substitution of the aqua ligands, a process that happens without undue dependence on the distance separating the Pt(II) centres in the complexes. This is despite a slight increase in the acidity of the protons of the aqua ligands brought about by an increased charge addition on decreasing the length of the linker.

Based on the *in vacuo* minimum energy structures of Table 2, also depicted in Fig. 2, and not withstanding conformation variability of the complexes, it is reasonable to assume that the symmetry of the complexes and the angles of elevation caused by the alkanediamine linker, including its electronic effects have an important bearing on the overall reactivity in these complexes. A look at the DFT calculated structures in Table 2 reveals that in the even-bridged complexes, the adopted C_{2h} point group symmetry places the Pt coordination spheres into two roughly parallel planes as depicted in Fig. 2. Viewed along the axis perpendicular to their mean planes containing the Pt atoms and the picolyl units, the bis(2-pyridylmethyl)amine chelates are located in mutually slip-up positions. The alkyldiamine linker lies at an inclination angle, α, that is inversely dependent on the length of the bridge. Relative to the plane containing one of the bis(2-pyridylmethyl)amine chelates, the linker projects the other chelate head at an angle which decreases sharply from 74.2° in **En** to 44.6° in **Dec** as documented in Table 3. When the chain length of the linker is increased, this has an effect of both increasing the projected distance locating the mean planes containing the chelates as well as their degree of mutual slip-up. In perspective, the chelates in **En** show a marked degree of aerial overlap and are separated by an elevation distance of only 3.63 Å, while those in **Dec** are well separated by as much as 9.16 Å (for an illustration refer also Fig. 2). Since this slip-up of coordination spheres occurs in one of the directions of approach of the nucleophile, it becomes evident that for complexes with a C_{2h} point group symmetry, the length of the linker controls the extent of steric disposition mutually imposed on one side of the Pt square-planar coordination sphere. This happens on the same side bearing the inclined linker. When the chain length is short, this imposes a stronger aerial steric influence on the same side of the metal chelate in the direction of the axially incoming nucleophile. Thus, from a view taken perpendicular to the planes containing the square-planar chelates in **En** and other complexes of shorter bridges, it is observed that one of the sides bearing the linking bridge at each Pt center is markedly blocked by the other metal chelate headgroup from a direct attack by the nucleophile as compared to **Dec** and other analogues of longer chain length. This kind of imposed steric hindrance is likely to be the dominant factor accounting for the difference in reactivity in the complexes.

Our results also suggest that this kind of steric influence controlled by the symmetry dictated by the linker piece is more important in the complexes bridged by an alkanediamine of shorter chain length. The steric influences decrease proportionally as the chain length is increased from **En** to **Hex**. This causes a proportional increase in reactivity from **En** up to **Hex**. Beyond **Hex**, any further increase in chain length does not result in significant changes in the elevation angles of the linker bridges and its projected effects on the reactivity of the complexes. As a result of this, the reactivity of **Hex**, **Oct** and **Dec** for the simultaneous displacement of the aqua ligands by the thioureas remains high and comparable to each other.

In the absence of this kind of steric imposition, as is the case for **Prop** where the Pt coordination spheres are near-orthogonal, other factors become more important in controlling reactivity of the Pt centers. As shown in Fig. 2, the calculated structure of **Prop** has two Pt atoms lying almost in near-orthogonal planes with no meaningful mutual shielding as a result of its C_{2v} symmetry. It is possible that the C_{2v} symmetry of **Prop** which draws the shape of the complex into a bowl-like cage,[36] can mediate in the entrapment of incoming nucleophiles aided by solvent molecules through the well known cage effect.[37] In keeping with the principles of the collision theory, this can increases the frequency of collisions between the Pt atoms and the entrapped nucleophiles within the overlooking faces of the bowl-shaped enclave. The result is a dramatic increase in the collision fraction, leading to more fruitful collisions. Conceivably, nucleophile-metal complex encounter pairs confined in a caged cleft can acquire sufficient energy to surmount the energy barrier. It thus stabilizes the transition state relative to the ground state. This stabilization is likely to depend on the depth of the cage.

To infer on the depth of the cleft, we measured the hinge angle, β, formed by the mean planes of the overlooking square-planar faces of the **Prop** as shown in its calculated structure in Fig. 2, such that its bisector passes through the central carbon of its propanediamine linker. The angle comes to 124°. This acute 'bowling' angle creates a cage of significant projected depth, enough to entrap axially approaching nucleophiles. Solvent molecules aid the entrapment process. Thus, deep and narrow bowled cages will increase the frequency of collisions. This is a likely explanation of the unusual high reactivity of **Prop** confirmed in this study and first observed by van Eldik and his group.[14a] When the rate constant for **Prop** determined in this study is combined to the rate constants for **Pen** and **Hep** from a previous study[14c] for tu as the entering nucleophile, a trend opposite to that recorded for the even-bridged complexes is observed. The second-order rate constant, $k_{2(1^{st})}$, increases monotonically from **Hep** (577 ± 5 M^{-1} s^{-1})[14c] through **Pen** (765 ± 10 M^{-1} s^{-1})[14c] to **Prop** (1033 ± 7 M^{-1} s^{-1}) in line with an increase in the entrapment effect as the basal width of the bowl is shortened. From this data, it is also clear that tuning the reactivity of dinuclear complexes with bis(2-pyridylmethethyl)amine chelate headgroups *via* varying the chain length of their alkanediamine linker will be more pronounced in the odd-bridged complexes than in their related even-bridged analogues due to a combination of the absence of steric dispositions and the profound entrapment effect of their cage structures.

The deceleration in the rate of substitution in going from the monomeric **bpma** to the **En** and **But** dinuclear complexes is in support of the presence of axially imposed steric influences on their Pt coordination spheres conferred as a result of their shorter and markedly inclined linkers. As the length of the linker is increased to **Hex**, this steric imposition is further decreased. At the same time, an increase in the number of CH_2 groups along the series causes an increase in electron density in the linker and hence the σ-inductive effect[14d] towards each Pt center. This, together with a higher charge of +4 causes a marginal increase in the reactivity of **Hex** compared to **bpma**. However, any further decrease in steric imposition along the series beyond **Hex** is not accompanied by

additional reactivity advantage over **bpma** as would be expected on the basis of a higher charge of +4 and a steady increase in the positive σ-inductive effects[14d] of the CH_2 groups towards the metal centers. Thus, an increase in the number of CH_2 groups from six in **Hex** to ten in **Dec** causes only a marginal increase in reactivity of about 1.6 (tu and dmtu) and 1.04 (tmtu). This is in spite of a slight elongation and weakening of the Pt-OH_2 bond (Table 3) as the chain length increases from **En** to **Dec**. It seems likely that this factor plays a subdued role in controlling reactivity in this series of complexes.

A common observation in the reactivity of these complexes is a second substitution step that proceeds at an invariably slowly rate of about two order of magnitude slower than for the simultaneous displacement of the aqua ligands. This step is less sensitive to the structural changes emanating from the linking diamino bridge. The behavior is consistent with a substitution step involving dechelation of one of the pyridyl units of the non-labile bis(2-pyridylmethethyl)amine chelate ligand as proposed in a previous study.[14c] It can possibly be due to the increased constraints poised on the incoming nucleophiles as they displace the coordinated pyridyl ligand at an already hindered Pt centre in the transition state.

The trend in the magnitude of the second-order rate constants (Table 4) for the substitution of the aqua ligands by the four nucleophiles (tu, dmtu, tmtu and I^-) is similar to that reported for **bpma** by Jaganyi *et al.*[20a,33a] These values show that the iodide nucleophile reacts about 50 times faster than the most reactive neutral nucleophiles (tu and dmtu). This reactivity difference can be explained on the basis of the strong electrostatic attraction forces between the anionic iodide nucleophile and the dicationic headgroups aided by the highly polarizability of this nucleophile. It is well documented that soft (polarizable) nucleophiles favour soft substrates like the Pt(II) ion resulting in superior reactivity.

The results of Table 5 shows that the activation entropies ($\Delta S^{\neq}_{(1^{st}/2^{nd})}$) are large and negative while the activation enthalpies ($\Delta H^{\neq}_{(1^{st}/2^{nd})}$) are low and positive. All this is in full support of an associative mechanism well known for d^8 square planar metal complexes.[38-41] The acceleration of the reactions by pressure and hence the negative volumes of activation ($\Delta V^{\neq}_{(1^{st})}$) measured in this study further support this mode of activation. Of note, are the large and more negative values for the volumes of activation measured for the reactions between **Prop** and the studied nucleophiles (tu and tmtu). It is an indication that the first reaction step for **Prop** proceeds *via* a more compact transition state when compared to other complexes. This is consistent with the proposed cage effect as discussed before. The collapse in volume in the transition state is mediated by the constraints of the entrapment effect and is therefore more negative when compared to the values of the other complexes.

Conclusions

This study has demonstrated that the symmetry elements of the dinuclear complexes with bis(2-pyridylmethyl)amine chelate headgroups as well as the length of the α,ω-alkanediamine linker can tune the reactivity of the complexes to some extent. For complexes with C_{2h} symmetry, their reactivity increases with increasing chain length of the α,ω-alkanediamine bridges to some point beyond which it levels off. This is attributed to the unblocking of axial steric impositions on one face of the Pt(II) square-planar coordination sphere conferred by the coordination sphere of the other Pt center in their C_{2h} slip-up sandwich molecular structures. This kind of mutual steric imposition reaches its limit of influence on reactivity in the **Hex** complex. When the complexes are bridged by an α,ω-alkanediamine linker bearing an odd number of carbon atoms as in the case of **Prop**, a cage effect evolving from the adopted bowl-shaped molecular structures controls reactivity. As a result of this, a significant entrapment effect on incoming nucleophiles take place inside the cavity of the bowl, more so in the acute-angled bowl of **Prop** causing an unusually high reactivity in this complex when compared to the rest of the complexes.

An observed second substitution step, confirmed by ^{1}H NMR spectroscopy for the reaction between the monomeric and monofunctional **bpma** and tu, indicates that all the subsequent reaction steps which are observed in the analogous homotopic dinuclear complexes with common bis(2-pyridylmethyl)amine chelate headgroups are in fact the dechelations of one of one of their *cis*-coordinated pyridyl units. Given the high nucleophilicity of the sulfur bearing thiourea nucleophiles at the Pt metal centers, it is no surprise why the thermodynamically stable bis(2-pyridylmethyl)amine chelate system is partially labilized and thus undergoes dechelation. However, no evidence of degradation of the crucial α,ω-alkanediamine linker was observed for all dinuclear complexes.

Acknowledgements

We gratefully acknowledge financial support from the University of KwaZulu-Natal and the National Research Foundation (NRF, Pretoria). We are indebted to the Alexander von Humboldt Foundation for the kind donation of the UV-Visible spectrophotometer. SH and RvE gratefully acknowledge continued support from the Deutsche Forschungsgemeinschaft.

References

1 E. Wong and C. M. Giandomenico, *Chem. Rev.*, 1999, **99**, 2451.
2 N. J. Wheate and J. G. Collins, *Coord. Chem. Rev.*, 2003, **241**, 133.
3 J. Reedijk, *Chem. Rev.*, 1999, **99**, 2499.
4 E. R. Jamieson and S. J. Lippard, *Chem. Rev.*, 1999, **99**, 2467.
5 N. Farrell, S. G. De Almeida and K. A. Skov, *J. Am. Chem. Soc.*, 1988, **110**, 5018.
6 N. Farrell, *Comments Inorg. Chem.*, 1995, **16**(6), 373.
7 M. E. Oehlsen, Y. Qu and N. Farrell, *Inorg. Chem.*, 2003, **42**, 5498.
8 (*a*) N. Farrell, in *Platinum-based Drugs in cancer Therapy*, 2000, L. R. Kelland and N. Farrell, (Ed.), Humana Press, Totowa, 321; (*b*) T. D. McGregor, Z. Balcarova, Y. Qu, M. C. Tran, R. Zaludova, V. Brabec and N. Farrell, *J. Biol. Inorg. Chem.*, 1999, **77**, 43.
9 V. Brabec and J. Kasparková, J., *Drug Resist. Updates*, 2005, **8**, 131.
10 J. Kasparková, O. Vraná, N. Farrell and V. Brabec, *J. Biol. Inorg. Chem.*, 2004, **98**, 1560.
11 N. Summa, J. Maigut, R. Puchta and R. van Eldik, *Inorg. Chem.*, 2007, **46**, 2094.
12 V. Vacchina, L. Torte, C. Allievi and R. Lobeinski, *J. Anal. At. Spectrom.*, 2003, **18**, 884.
13 D. Jaganyi, V. M. Munisamy and D. Reddy, *Int. J. Chem. Kinet.*, 2006, **38**, 202.
14 (*a*) A. Hofmann and R. van Eldik, *Dalton Trans.*, 2003, 2979; (*b*) H. Ertürk, A. Hofmann, R. Puchta and R. van Eldik, *Dalton Trans.*, 2007, 2295; (*c*) H. Ertürk, J. Maigut, R. Puchta and R. van Eldik, *Dalton Trans.*, 2008, 2759; (*d*) H. Ertürk, R. Puchta and R. van Eldik, *Eur. J. Inorg. Chem.*, 2009, 1334.
15 J. W. Williams, Y. Qu, H. Bulluss, E. Alvorado and N. Farrell, *Inorg. Chem.*, 2007, **46**, 5820.

16 (*a*) N. Summa, J. Maigut, W. Schiessl, R. Puchta, N. van Eikema-Hommes and R. van Eldik, *Inorg. Chem.*, 2006, **45**(7), 2948; (*b*) D. Reddy and D. Jaganyi, *Transition Met. Chem.*, 2006, **31**, 792; (*c*) M. Schmülling, A. D. Ryabov and R. van Eldik, *J. Chem. Soc., Dalton Trans.*, 1996, 1471; (*d*) M. J. Carter and J. K. Beattie, *Inorg. Chem.*, 1970, **9**, 1233.
17 (*a*) S. Komeda, G. V. Kalayda, M. Lutz, A. L. Spek, T Sato, M. Chikuma and J. Reedijk, *J. Med. Chem.*, 2003, **46**, 1210; (*b*) G. V. Kalayda, S. Komeda, K. Ekeda, T. Sato, M. Chikuma and J. Reedijk, *Eur. J. Inorg. Chem.*, 2003, 4347.
18 (*a*) S. Komeda, M. Lutz, A. L. Spek, M. Chikuma and J. Reedijk, *Inorg. Chem.*, 2000, **39**, 4230; (*b*) S. Komeda, M. Lutz, A. L. Spek, Y. Yamanaka, T. Sato, M. Chikuma and J. Reedijk, *J. Am. Chem. Soc.*, 2002, **124**, 4738.
19 S. L. Woodhouse and L.M. Rendina, *Chem. Commun.*, 2001, 2464(*a*) N. J. Wheate, C. Cullinane, L. K. Webster and J. G. Collins, *Anticancer Drug Design*, 2001, 1691.
20 (*a*) D. Jaganyi, A. Hofmann and R. van Eldik, *Angew. Chem., Int. Ed.*, 2001, **40**, 1680; (*b*) Z. D. Bugarčić, G. Liehr and R. van Eldik, *J. Chem. Soc., Dalton Trans.*, 2002, 951.
21 A. Sato, Y. Mori and T. Lida, *Synthesis*, 1992, 539.
22 Z. D. Bugarčić, B. V. Petrović and R. Jelić, *Transition Met. Chem.*, 2001, **26**, 668.
23 A. Hofmann, D. Jaganyi, O. Q. Munro, G. Liehr and R. van Eldik, *Inorg. Chem.*, 2003, **42**, 1688.
24 R. van Eldik, W. Gaede, S. Wieland, J. Kraft, M. Spitzer and D. A. Palmer, *Rev. Sci. Instrum.*, 1993, **64**, 1355.
25 (*a*) R. A. Friesner, *Chem. Phys. Lett.*, 1985, **116**, 39; (*b*) R. A. Friesner, *Annu. Rev. Phys. Chem.*, 1991, **42**, 341.
26 (*a*) Spartan 04, Wavefunction, Inc., 18401 von Karman Avenue, Suite 370, Irvine, CA, 92612, USA; Q-Chem, Inc, The Design Center, suite 690, 5001, Baum Blvd., Pittsburgh, 15213, USA, 2004. http://www.wavefun.com/; (*b*) K. Kong, C. A. White, A. I. Krylov, C. D. Sherrill, R. D. Adamson, T. R. Furlani, M. S. Lee, A. M. Lee, S. R. Gwaltney, T. R. Adams, C. Ochsenfeld, A. T. B. Gilbert, G. S. Kedziora, V. A. Rassolov, D. R. Maurice, N. Nair, Y. Shao, N. A. Besley, P. E. Maslen, J. P. Dombroski, H. Daschel, W. Zhang, P. P. Korambath, J. Baker, E. F. C. Byrd, T. van Voorhuis, M. Oumi, S. Hirata, C. P. Hsu, N. Ishikawa, J. Florian, A. Warshel, B. G. Johnson, P. M. W. Gill and B. G. Pople, *J. Comput. Chem.*, 2000, **21**, 1532.
27 (*a*) A. D. Becke, *J. Chem. Phys.*, 1993, **98**, 5648; (*b*) C. Lee, W. Yang and R. G. Parr, *Phys. Rev.*, 1998, **B37**, 785.
28 (*a*) P. C. Hariharan and J. A. Pople, *Chem. Phys. Lett.*, 1972, **16**, 217; (*b*) P. J. Hay and W. R. Wadt, *J. A. Chem. Phys. Lett.*, 1985, **82**, 299.
29 Origin7.5™ SRO, v7.5714 (B5714), Origin Lab Corporation, Northampton, One, Northampton, MA, 01060, USA, 2003.
30 D. Jaganyi and F. Tiba, *Transition Met. Chem.*, 2003, **28**, 803.
31 (*a*) B. Pitteri, G. Annibale, G. Marangoni, V. Bertolasi and V. Ferretti, *Polyhedron*, 2002, **21**, 2283; (*b*) ConQuest *v*1.9, 2006, Cambridge Crystallographic Data Centre, 12 Union Road, Cambridge, CB21EZ, United Kingdom.
32 (*a*) C. F. Weber and R. van Eldik, *Eur. J. Inorg. Chem.*, 2005, 4755; (*b*) B. Pitteri, M. Bortoluzzi and G Marangoni, *Transition Met. Chem.*, 2005, **30**, 1008.
33 (*a*) D. Jaganyi, F. Tiba, O. Q. Munro, B. Petrović and Z. D. Bugarčić, *Dalton Trans.*, 2006, 2943; (*b*) Z. D. Bugarčić, G. Liehr and R. van Eldik, *Dalton Trans.*, 2001, 951.
34 S. M. Owen and A. T. Bruker, *A Guide to Modern Inorganic Chemistry*, Longman Scientific & Technical, Essex, England, 1991, pp. 193-194.
35 A. Mambanda, D. Jaganyi and O. Q Munro, *Acta Crystallogr., Sect. C: Cryst. Struct. Commun.*, 2007, **63**, o676.
36 U. Fekl and R. van Eldik, *Inorg. Chem.*, 2001, **40**, 3247.
37 P. W. Atkins, *Physical Chemistry*, 6th Ed., Oxford University Press, Oxford, 1998, pp. 825-827.
38 M. L. Tobe and J. Burgess, *Inorganic Reaction Mechanisms*, Addison Wisey, Longman Ltd., Essex, 1999, pp. 30–33; 70–112.
39 J. D. Atwood, *Inorganic and Organometallic Reaction Mechanisms*, 2nd Ed., Wiley-VCH, NY, 1997, pp. 43–61.
40 R. G. Wilkins, *Kinetics and Mechanism of Reactions of Transition Metal Complexes*, 2nd Ed., VCH, Weinheim, 1991, pp. 199–201.
41 F. Basolo and R. G. Pearson, *Mechanism of Inorganic Reactions*, 2nd Ed., Wiley, New York, 1967, pp. 80–115.

